AGU PUBLICATIONS

JGR

Journal of Geophysical Research: Biogeosciences

RESEARCH ARTICLE
10.1002/2014JG002623

Key Points:
- Land-surface models produce subdaily patterns of latent heat flux error
- Error patterns are characterized by the stomatal conductance formulation used
- Current models lack a mechanism to simulate hysteretic transpiration

Correspondence to:
A. M. Matheny,
matheny.44@osu.edu

Citation:
Matheny, A. M., et al. (2014), Characterizing the diurnal patterns of errors in the prediction of evapotranspiration by several land-surface models: An NACP analysis, *J. Geophys. Res. Biogeosci.*, *119*, 1458–1473, doi:10.1002/2014JG002623.

Received 17 JAN 2014
Accepted 26 JUN 2014
Accepted article online 30 JUN 2014
Published online 31 JUL 2014

Characterizing the diurnal patterns of errors in the prediction of evapotranspiration by several land-surface models: An NACP analysis

Ashley M. Matheny[1], Gil Bohrer[1], Paul C. Stoy[2], Ian T. Baker[3], Andy T. Black[4], Ankur R. Desai[5], Michael C. Dietze[6], Chris M. Gough[7], Valeriy Y. Ivanov[8], Rachhpal S. Jassal[4], Kimberly A. Novick[9], Karina V. R. Schäfer[10], and Hans Verbeeck[11]

[1]Department of Civil, Environmental, and Geodetic Engineering, Ohio State University, Columbus, Ohio, USA, [2]Department of Land Resources and Environmental Sciences, Montana State University, Bozeman, Montana, USA, [3]Atmospheric Science Department, Colorado State University, Fort Collins, Colorado, USA, [4]Faculty of Land and Food Systems, University of British Columbia, Vancouver, British Columbia, Canada, [5]Center for Climatic Research, University of Wisconsin-Madison, Madison, Wisconsin, USA, [6]Department of Earth and Environment, Boston University, Boston, Massachusetts, USA, [7]Department of Biology, Virginia Commonwealth University, Richmond, Virginia, USA, [8]Department of Civil and Environmental Engineering, University of Michigan, Ann Arbor, Michigan, USA, [9]School of Public and Environmental Affairs, Indiana University, Bloomington, Indiana, USA, [10]Department of Biological Sciences, Rutgers University, Newark, New Jersey, USA, [11]Department of Applied Ecology and Environmental Biology, Ghent University, Ghent, Belgium

Abstract Land-surface models use different formulations of stomatal conductance and plant hydraulics, and it is unclear which type of model best matches the observed surface-atmosphere water flux. We use the North American Carbon Program data set of latent heat flux (LE) measurements from 25 sites and predictions from 9 models to evaluate models' ability to resolve subdaily dynamics of transpiration. Despite overall good forecast at the seasonal scale, the models have difficulty resolving the dynamics of intradaily hysteresis. The majority of models tend to underestimate LE in the prenoon hours and overestimate in the evening. We hypothesize that this is a result of unresolved afternoon stomatal closure due to hydrodynamic stresses. Although no model or stomata parameterization was consistently best or worst in terms of ability to predict LE, errors in model-simulated LE were consistently largest and most variable when soil moisture was moderate and vapor pressure deficit was moderate to limiting. Nearly all models demonstrate a tendency to underestimate the degree of maximum hysteresis which, across all sites studied, is most pronounced during moisture-limited conditions. These diurnal error patterns are consistent with models' diminished ability to accurately simulate the natural hysteresis of transpiration. We propose that the lack of representation of plant hydrodynamics is, in part, responsible for these error patterns.

1. Introduction

Evapotranspiration (ET) accounts for 60% of precipitated water in some catchments and up to 95% in others, comprising the largest component of the terrestrial hydrologic cycle [*Fisher et al.*, 2005; *Ford et al.*, 2007; *Jasechko et al.*, 2013; *Katul et al.*, 2012]. *Jasechko* [2013] has recently shown that more than 80% of terrestrial ET must be partitioned to transpiration to maintain a mass balance between plant transpiration and CO_2 uptake. Transpiration couples the carbon and water cycles and acts as a principal feedback between the land surface and atmosphere. Furthermore, stomatal conductance controls transpiration rates and acts as a princpal control to the surface energy redistribution and thus couples transpiration with sensible heat and convection at the planetary surface layer. It is therefore crucial to understand its dynamics [*Savabi and Stockle*, 2001]. Concomitant to transpiration, terrestrial ecosystems take up an average of approximately 120 Pg of carbon annually, providing a critical sink for atmospheric CO_2 [*Beer et al.*, 2010; *Pan et al.*, 2011]. C uptake rates are also limited by stomatal conductance. With global and regional temperature increases and a potential rise of the variation in regional precipitation patterns, the ability to accurately model transpiration is essential to predicting land surface-climate change feedback in terms of heat, water, and carbon exchange [*Allen et al.*, 2010; *Berry et al.*, 2010; *Choat et al.*, 2012; *Huntington et al.*, 2009; *Jasechko et al.*, 2013; *Niyogi et al.*, 2009; *Wu et al.*, 2012].

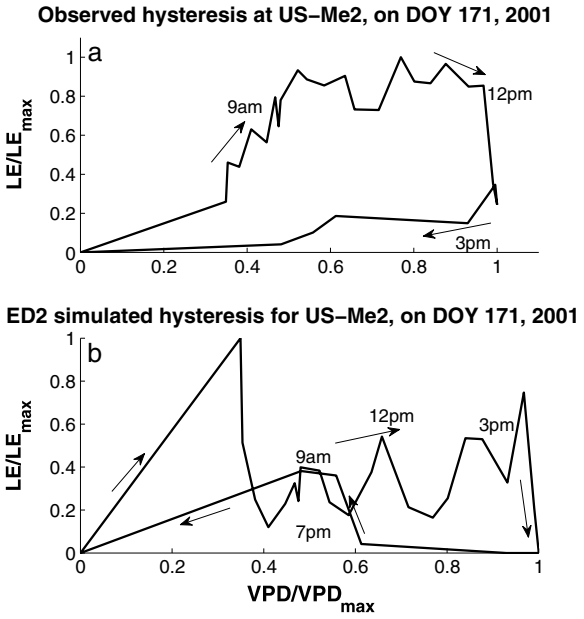

Figure 1. Examples of observed hysteresis at (a) US-ME2 on day of year 171 of 2001 and model-"simulated" hysteresis from (b) ED2 for the same day. Arrows and times indicate the direction of the hysteretic cycle. LE_{max} and VPD_{max} are the respective maxima for the day shown.

Plants balance the uptake of CO_2 required for photosynthesis with the need to maintain sufficient moisture levels inside the leaf. Leaves close their stomata to avoid decreases in leaf water potential that could lead to desiccation or catastrophic cavitation within the xylem system [*Brodribb and Holbrook*, 2003, 2006, 2007; *Brodribb and Cochard*, 2008; *Tyree and Zimmermann*, 2002; *Zimmerman*, 1983]. Stomata operate dynamically to regulate water loss and C uptake, and this regulation—ultimately a function of controls over guard cell function—is related to a number of external environmental variables including incoming solar radiation, ambient CO_2 concentration, temperature, humidity, and soil water availability and internal physiological variables such as CO_2 concentration within the leaf, abscisic acid (ABA) concentration within the leaf, and leaf water potential [*Ball*, 1988; *Sperry et al.*, 2002; *Tyree and Zimmermann*, 2002]. Regulation of stomatal conductance due to leaf-level water stress is known to control transpiration when the soil is dry or when vapor pressure deficit (VPD) is large but can also impact stomatal apertures under conditions of adequate soil moisture and lower evaporative demand if depletion of water storage in the leaves occurs at a faster rate than recharge through roots, stems, and branches [*Brodribb and Holbrook*, 2004; *McCulloh et al.*, 2012; *Sperry et al.*, 2002]. The imbalance, or lack thereof, between water demand in the leaf and water supply from the soil imposes hydrodynamic limitations on stomatal conductance [*Bohrer et al.*, 2005; *Damour et al.*, 2010; *McCulloh and Sperry*, 2005; *Thomsen et al.*, 2013; *Tyree and Sperry*, 1989; *Zhang et al.*, 2014].

Despite numerous advances in the understanding of water transport, current land surface and ecosystem models do not adequately resolve observed hydrodynamic phenomena within the plants [*Damour et al.*, 2010; *Egea et al.*, 2011]. At present, the most widely used models for stomatal conductance (g_s) are based on the net photosynthetic rate and environmental variables, most frequently photosynthetic active radiation (PAR) and relative humidity or VPD [e.g., *Ball et al.*, 1987; *Collatz et al.*, 1991; *Leuning*, 1995]. These models do not include a mechanistic link between leaf water potential and stomatal conductance but instead force water supply limitations through empirical parameterizations of the response of g_s to soil moisture at the root zone, representing a "conceptual" understanding of the soil control on plant water uptake [*De Kauwe et al.*, 2013]. This relationship is generally obtained through the use of a heuristic, Feddes-type or Jarvis-type parameterization [*Feddes et al.*, 1976; *Jarvis*, 1976], which describes threshold values of soil water potential, i.e., the onset of soil stress and the permanent wilting point, between which stomatal behavior leads to suppressed flux and gas exchange. Within this range of values, stomatal conductance declines linearly or sigmoidally with declining water availability. Alternatively, hydraulically based models for stomatal conductance link stomatal function to leaf water potential [*Bohrer et al.*, 2005; *Janott et al.*, 2011; *Tuzet et al.*, 2003] but typically require extensive knowledge of plant hydraulic parameters such as a species' threshold for cavitation, hydraulic and tree architecture, tree water storage capacity, or the cumulative root-to-leaf resistance to water transport; all of which are difficult to measure, parameterize, and implement over across multiple species, canopy and crown structures, and plant functional types. Although these hydrodynamic models provide a more physically realistic description of the plant hydraulic system and thus can simulate the effects of diurnal water stress and drought limitations on transpiration, they have not been widely incorporated in land-surface models to date [*Damour et al.*, 2010; *Egea et al.*, 2011; *Hickler et al.*, 2006].

A hallmark feature of plant hydrodynamics is the daily hysteresis of transpiration (Figure 1). For the same VPD, plants transpire more during the morning, when internal storage levels are high, than during the afternoon

when water storage in the stem is depleted [*Bohrer et al.*, 2005; *Phillips et al.*, 2003; *Verbeeck et al.*, 2007a; *Zhang et al.*, 2014]. We hypothesize that models will produce patterns of diurnal error that are representative of the missing mechanistic representation of the physiological response to plant hydrodynamics, namely, a hysteresis, as fluxes are underestimated during morning and overestimated in the afternoon. These patterns will be characteristic of the form and parameterization of the stomatal conductance model, the manner in which water stress limitations are enforced, and the ecosystem type, all of which are related to the features of plant hydrodynamics noted above. Errors in model predictions of stomatal conductance translate directly into errors in the prediction of transpiration and therefore evapotranspiration and latent heat flux (LE), the heat flux associated with the vaporization of water. Furthermore, when models are well parameterized for the long-term overall transpiration (daily, weekly, or monthly), we expect to find an underestimation of transpiration during the morning and early afternoon to compensate for the afternoon-early evening overestimation. It is likely, therefore, that errors in LE will additionally lead to errors in the sensible heat flux (H) on account of incorrect partitioning of the turbulent flux terms in the surface energy balance. Overestimations of afternoon evapotranspiration will cause afternoon temperature to appear lower, thus causing a "damping" effect on the modeled H. Errors in resolving stomatal conductance will also influence a model's ability to correctly predict photosynthesis and therefore may propagate into the model's predictions of gross primary productivity (GPP) [*Schaefer et al.*, 2012] and net ecosystem exchange (NEE) [*Dietze et al.*, 2011; *Schwalm et al.*, 2010; *Stoy et al.*, 2013].

The specific objectives of our study are as follows: (1) characterize the patterns of intradaily errors in model-simulated LE; (2) if typical error patterns exist, determine whether these patterns are typical of site characteristics (biome, mean annual rainfall, soil texture, and leaf area index) or model formulation (i.e., the parameterization of stomatal function and water stress); and (3) determine the extent to which errors in LE are propagated into errors in carbon flux. We test these predictions by comparing simulation results from 9 commonly used land-surface models with observations from 25 eddy-covariance tower sites of different ecosystem types. The data were collected as part of the North American Carbon Program (NACP).

2. Methods

2.1. Data Sources and Preparation

This study uses a large-scale intercomparison between eddy-covariance observations of surface H, LE, and CO_2 fluxes from multiple sites and simulation results from an ensemble of land-surface models to characterize the patterns of intradaily error in simulated LE. The North American Carbon Program (NACP) (http://www.nacarbon.org/nacp/) site-level interim synthesis project began in 2008 and was developed with the purpose of comparing eddy-covariance measurements and model outputs across different biomes [*Schwalm et al.*, 2010]. One of the purposes of the NACP synthesis was to compare the differences between modeled and observed values for as many site model pairs as possible as a way of assessing the confidence of observed and modeled data and of identifying ways to improve the confidence of both simulated and empirical measurements [*Dietze et al.*, 2011; *Richardson et al.*, 2012; *Schaefer et al.*, 2012; *Stoy et al.*, 2013]. In this study, we used a subset of sites and models that is included in the NACP interim site synthesis data set. Models were run in accordance with the NACP protocol (http://nacp.ornl.gov/docs/Site_Synthesis_Protocol_v7.pdf). We selected all sites for which flux data were available from at least 10 models and all models that provided simulation data on a subdaily basis for a minimum of 20 sites that encompass a range of North American ecosystem types in boreal to subtropical climate zones. Tables 1 and 2 list the sites ($n = 25$) and models ($n = 9$) included in our analysis, although not all models were run for every site. Overall, we analyze 209 model site pairs. It is important to acknowledge that under the NACP, modelers were given the choice of which sites to run or not run.

We used half hourly or hourly observations, depending on the averaging time available from the site, of LE, H, and NEE for all the sites to compare with the models' simulation results for the same sites. These data are based on the contributions by site principal investigators (PIs) from the Ameriflux and Fluxnet Canada networks. As this paper focuses on the effects of hydrodynamic regulation of stomatal conductance, we used only data from the growing season, when transpiration was expected to be an important component of the site water balance and dominate the total evapotranspiration flux. We did not attempt to partition LE into transpiration and evaporation components [*Stoy et al.*, 2006]. While models or additional measurements may

Journal of Geophysical Research: Biogeosciences 10.1002/2014JG002623

Table 1. Site Summary: Site Details (Latitude, Longitude, Elevation, Soil Class, and International Geosphere-Biosphere Programme (IGBP) for U.S. Sites From http://public.ornl.gov/ameriflux/ and for Canada Sites From http://fluxnet-canada.ccrp.ec.gc.ca/ Mean Annual Rainfall as Calculated by *Schwalm et al.* [2010]

Site	Name	Latitude	Longitude	Elevation (meter above sea level)	Annual Precipitation (mm)	Years	Soil Class	IGBP	Reference
CA-Ca1	Campbell River	49.87	−125.33	300	1256	1998–2006	Sandy loam	Evergreen Needleleaf Forests (ENF)	*Schwalm et al.* [2007]
CA-Gro	Groundhog River	48.22	−82.16	200	427	2004–2006	Sandy loam	Mixed Forests (MF)	*McCaughey et al.* [2006]
CA-Let	Lethbridge	49.71	−112.94	960	335	1997–2007	Clay loam	Grasslands (GRA)	*Flanagan et al.* [2002]
CA-Oas	Southern Study Area (SSA) Old Aspen	53.63	−106.20	530	460	1997–2006	Loam	Deciduous Broadleaf Forests (DBF)	*Barr et al.* [2004]
CA-Obs	SSA Old Black Spruce	53.99	−105.12	629	470	2000–2006	Sandy loam	ENF	*Griffis et al.* [2003]
CA-Ojp	SSA Old Jack Pine	53.92	−104.69	579	461	2000–2006	Sand	ENF	*Griffis et al.* [2003]
CA-Qfo	Quebec Mature Forest	49.69	−74.34	382	819	2004–2006	Sandy loam	ENF	*Bergeron et al.* [2007]
US-ARM	Lamot S. Great Plains	36.61	−97.49	310	629	2000–2007	Silty clay loam	Croplands (CRO)	*Fischer et al.* [2007]
US-Dk3	Duke Forest	35.98	−79.09	163	1126	1998–2005	Sandy loam	ENF	*Siqueira et al.* [2006]
US-Ha1	Harvard Forest	42.54	−72.17	303	1122	1991–2006	Sandy loam	DBF	*Urbanski et al.* [2007]
US-Ho1	Howland Forest	45.20	−68.74	60	818	1996–2004	Sandy loam	ENF	*Richardson et al.* [2009]
US-IB2	Batavia Prairie	41.84	−88.24	227	818	2004–2007	Silty clay loam	GRA	*Post et al.* [2004]
US-Me2	Metolius Intermediate	44.45	−121.56	1253	434	2002–2007	Sand	ENF	*Thomas et al.* [2009]
US-MMS	Morgan Monroe State Forest	39.32	−86.41	275	1109	1999–2006	Clay loam	DBF	*Schmid et al.* [2000]
US-MOz	Missouri Ozark	38.74	−92.20	219	730	2004–2007	Silt loam	DBF	*Gu et al.* [2006]
US-Ne1	Mead Irrigated Maize	41.47	−96.48	361	832	2001–2006	Silty clay loam	CRO	*Verma et al.* [2005]
US-Ne2	Mead Irrigated Rotation	41.16	−96.47	361	823	2001–2006	Silty clay loam	CRO	*Verma et al.* [2005]
US-Ne3	Mead Rainfed Rotation	41.18	−96.44	361	627	2001–2006	Silty clay loam	CRO	*Verma et al.* [2005]
US-NR1	Niwot Ridge Forest	40.03	−105.55	3050	663	1998–2007	Clay	ENF	*Bradford et al.* [2008]
US-PFa	Park Falls/WLEF	45.95	−90.27	485	736	1995–2005	Sandy loam	MF	*Davis et al.* [2003]
US-Syv	Sylvania Wilderness	46.24	−89.35	540	700	2001–2006	Sandy loam	MF	*Desai et al.* [2005]
US-Ton	Tonzi Ranch	38.43	−120.97	177	549	2001–2007	Silt loam	Woody Savanna (WSA)	*Ma et al.* [2007]
US-UMB	U of M Biological Station	45.56	−84.71	234	629	1999–2006	Loamy sand	DBF	*Gough et al.* [2013]; *Nave et al.* [2011]
US-Var	Vaira Ranch	38.41	−120.95	129	563	2000–2007	Silt loam	GRA	*Ma et al.* [2007]
US-Wcr	Willow Creek	45.81	−90.08	520	712	1998–2006	Sandy loam	DBF	*Cook et al.* [2004]

Table 2. Summary of Models: Stomatal Conductance Formulation, Water Stress Function and Moisture Limitation Enforcement, Temporal Resolution, Phenology Scheme, and GPP Methodology

Model	Stomata Parameterization	Water Stress Function	Temporal Resolution	Canopy Phenology	GPP	Reference
Can IBIS	*Collatz et al.* [1991]	Jarvis type, direct and indirect	Half hourly	Prognostic	Enzyme Kinetic	*Kucharik et al.* [2000]
CN-CLASS	*Ball et al.* [1987]	Feddes type, direct	Half hourly	Prognostic	Enzyme Kinetic	*Arain et al.* [2006]
Ecosys	*Grant et al.* [2006]	Turgor potential, direct	Hourly	Prognostic	Enzyme Kinetic	*Grant et al.* [2006]
ED2	*Leuning* [1995]	Bucket model, direct	Half hourly	Prognostic	Enzyme Kinetic	*Medvigy et al.* [2009]
ORCHIDEE	*Ball et al.* [1987]	Jarvis type, indirect	Half hourly	Prognostic	Enzyme Kinetic	*Verbeeck et al.* [2011]
SiB3	*Collatz et al.* [1991]	Feddes type, indirect	Half hourly	Prescribed	Enzyme Kinetic	*Baker et al.* [2008]
SibCASA	*Collatz et al.* [1991]	Jarvis type, indirect	Half hourly	Prescribed	Enzyme Kinetic	*Schaefer et al.* [2008]
SSiB2	*Collatz et al.* [1991]	Jarvis type, indirect	Half hourly	Prescribed	Stomatal Conductance	*Sellers et al.* [1995]
Teco	*Ball et al.* [1987]	Feddes type, direct	Hourly	Prognostic	Stomatal Conductance	*Weng and Luo* [2008]

be able to provide the separate estimates for these two components of the total LE, the flux sites reported only direct measurements of total LE. In an effort to avoid additional error due to partitioning uncertainty, we discuss only errors regarding model predictions of total evapotranspiration, in terms of LE, during a continuous period defined by the peak of the growing season when we expect transpiration from vegetation to be the dominant term of evapotranspiration. The length of the growing season was determined using the carbon flux phenology approach [*Garrity et al.*, 2012] from gap-filled observational NEE provided in the NACP data set. We further focused on the peak growing seasons by using observations during periods when carbon uptake flux was at least 50% of the peak 1 month moving average flux. It is worth noting that during the peak of the growing season, leaf area index is high at most of these sites (i.e., >3.0), such that the contribution of soil evaporation to the total ET should be minimal [*Oishi et al.*, 2008].

All flux observations in the data set were filtered to remove periods of low turbulent mixing, during which eddy-covariance measurements are inaccurate. We conducted that filtering using a site-specific friction velocity (u_*) threshold calculation following *Reichstein et al.* [2005]. Only actual observations (not gap filled) were used, and analysis was only conducted where observations were available. Carbon fluxes were provided as the net ecosystem exchange (NEE) of CO_2 and its components, gross primary productivity (GPP) and ecosystem respiration. GPP was modeled from observations of NEE and daytime respiration estimated by the relationship between nighttime NEE and microclimate variables by the site PIs contributing data to the NACP analysis.

Soil moisture and VPD were obtained from http://public.ornl.gov/ameriflux/ for U.S. sites and at http://fluxnet-canada.ccrp.ec.gc.ca/ for Canadian sites. In order to compare the amount of soil water available for plant uptake among sites, volumetric soil water content and site-specific soil properties were used to calculate the soil water matric potential, Ψ_s, following *Rawls et al.* [1982]. Soil characteristics provided by the Ameriflux and Fluxnet Canada websites were used to approximate soil texture used in the determination of soil water content at the permanent wilting point and field capacity following *Campbell and Norman* [1998]. Soil conditions were then divided on the basis of Ψ_s into three categorical levels, representing times when the soil was near the field capacity, near the permanent wilting point, and in the region of intermediate moisture conditions. VPD was divided to three categorical levels in a similar manner based on each site's seasonal mean daily VPD. Days for which the daily mean VPD fell within the highest 33% of the seasonal range of VPD for that site were considered "high-VPD" days; similarly, in "low-VPD" days, the mean daily VPD falls within the bottom 33%, and "intermediate VPD" refers to the middle 33%.

2.2. Analysis of Model Errors

Model outputs of LE were compared to observed data for all sites at a half hourly resolution. For the few sites where observations were provided in hourly time steps (US-Ha1, US-MMS, US-Ne1, US-Ne2, US-Ne3, US-PFa, and US-UBS), observations were linearly interpolated to half hourly. The daily cycle was interpreted on the basis of local time in all sites, and UTC timestamps were converted to local time where needed. Error was calculated as the difference between modeled and observed values for each half hour. Errors in *H*, GPP, and NEE were also calculated and analyzed for correlations with LE error.

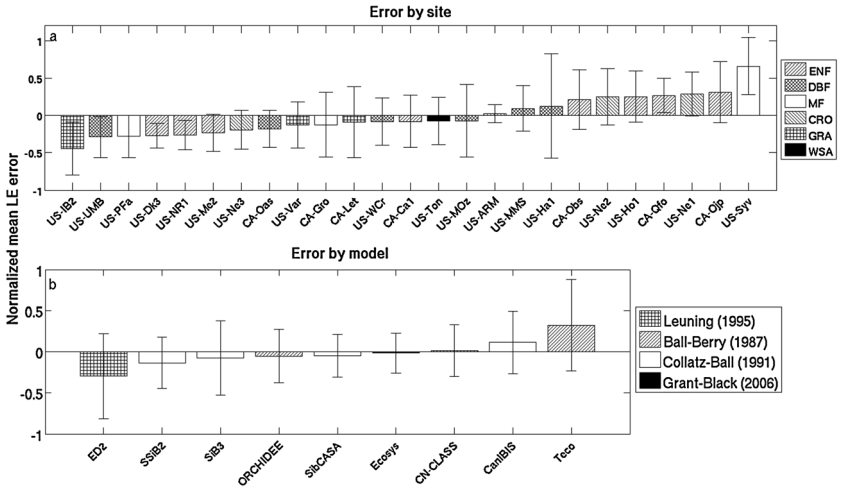

Figure 2. Average normalized growing season LE error across all models: (a) for each site studied and (b) across all sites for each model studied. Figure 2a patterns represent each site's IGBP classification: ENF–evergreen needleleaf forest, DBF–deciduous broadleaf forest, MF–mixed forest, CRO–crop, GRA–grassland, and WSA–woody savanna. Figure 2b patterns represent the stomatal conductance parameterization employed in each model. Error bars represent the standard deviation for (Figure 2a) each site among models and for (Figure 2b) each model among sites.

To determine the diurnal pattern of the errors, we calculated the mean error for each model site pair for every half hour of the day using only peak growing season data averaged over all days and years of observation at each site and normalized by the mean observed LE over all years for each site. We repeated the same analysis conditioned on the three levels (wet, intermediate, and dry) of soil water matric potential or VPD. Grand average errors in LE for each site model pair were calculated by averaging all normalized half hourly errors for the growing seasons in all years and all soil water matric potential/VPD conditions. The average daily error per model was calculated as the mean across all sites of the mean daily error, and the average daily error per site was calculated as the mean error across models. Sites were grouped based on ecosystem type and climate. Models were grouped based on the type of stomatal conductance parameterization scheme employed, the type of water stress function used, and to what terms in the stomata formulation water stress limitations were applied. Models that enforced water stress limitations in the calculation for g_s were considered to be "direct," and models that enforce limitations through the carboxylation capacity were considered to be "indirect" (Table 2).

2.3. Analysis of Hysteresis of the Diurnal Water Flux Cycle

Transpiration exhibits a distinct hysteresis in the diurnal pattern that can be seen by plotting LE as a function of VPD during the course of each individual day [*Chen et al.*, 2011; *O'Grady et al.*, 2008]. The plot traces a clockwise loop characteristic of the system's hysteresis (Figure 1a) [*Verbeeck et al.*, 2007a; *Zhang et al.*, 2014]. In this work, the "degree of hysteresis" of LE was defined as the integrated area encompassed by the loop. A (0,0) point, representing minimal nighttime transpiration, was included as a boundary condition to numerically close the loop and allow calculation of the loops' integrated interior area [*Novick et al.*, 2009]. Observed VPD and modeled LE were used to calculate the "model-simulated degree of hysteresis," shown as an example for the ED2 model at Metolius Intermediate field site, US-Me2, in Figure 1b. This metric of hysteresis was calculated for each day in each model or site data and then averaged across days, models, and sites. Degree of hysteresis was also averaged for each of the three soil water potential categories and VPD categories using the same categorical breakdown as discussed above based on the daily mean soil water matric potential and daily mean VPD.

3. Results and Discussion

3.1. Errors in Simulated LE at the Long (Seasonal) Time Scale

Models were evaluated by their ability to simulate LE across multiple sites representing a variety of ecosystems. The mean daily growing season errors across all sites for each model and across all models for each site are

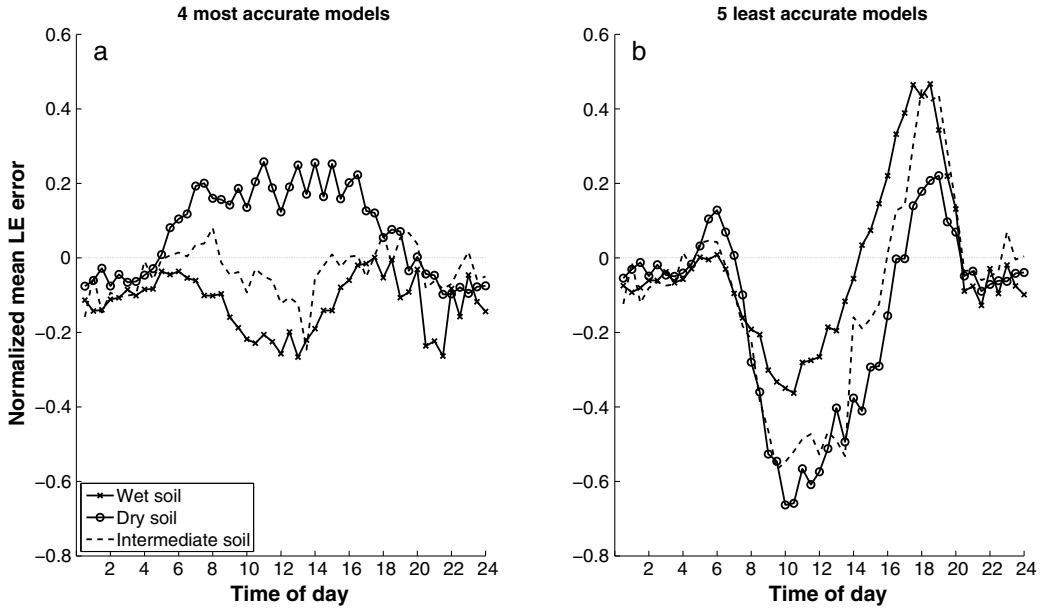

Figure 3. Diurnal model error patterns for (a) the four models with the smallest bias and (b) the five models with the largest bias. Error is broken down based on soil wetness conditions: soil wetness is near the field capacity ("wet soil"), soil moisture is near the permanent wilting point ("dry soil"), and soil conditions are in the intermediate ranges of conditions ("intermediate soil").

shown in Figure 2. No stomatal conductance formulation type was found to provide consistently the best or worst simulated LE across all sites or ecosystem types (Figure 2b). However, the model that used the Leuning [*Leuning*, 1995] formulation consistently produced an underestimation of LE, although this underestimation was not extreme in its magnitude relative to the mean errors of other parameterization approaches and may be due to factors other than the model for stomatal conductance. Overall, all models produced a rather good estimation of LE, with mean half hourly errors of less than 25% of the mean flux. The error of most models at most sites was less than 10% (Figure 2), similar to the range of error suggested for LE observations in flux sites [*Richardson et al.*, 2006]. The ecosystem type did not affect overall errors (Figure 2a). No significant correlations were found between mean growing season LE errors for each site and mean annual rainfall, elevation, mean annual temperature, ecosystem type, or leaf area index (data not shown). Errors in model-simulated LE were larger, and there were more variables when the daily average soil water content was moderate to low (Figure 3) and when the daily average VPD was moderate to high (VPD data not shown). This suggests that models have difficulties simulating the dynamics that cause stomata to close during moderate soil water content and are probably not driven by soil water availability limitation of transpiration. Models performed best at extreme conditions, for example, when conditions were very wet or when conditions are very dry and the stomata exhibit high resistance to gas/vapor flows. Larger errors in LE, in absolute terms, occurred during the peak hours of photosynthesis and transpiration (9 A.M. to 3 P.M., consistent with *Richardson et al.* [2006], i.e., when LE was largest).

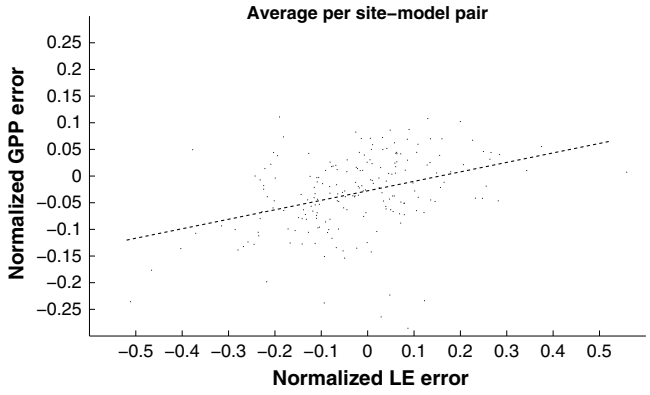

Figure 4. Average error in GPP versus average error in LE for each site model pair. Flux errors were normalized by the respective maximum error for each site model pair. $R^2 = 0.14$, slope = 0.18, and $P < 0.0001$.

3.2. Relationships Between LE and Carbon Flux Errors

Overall, errors in LE were found to have a positive linear correlation with errors in GPP; however, the amount of variation explained by this correlation was low (Figure 4). Although errors in

the modeled carbon flux may stem from a variety of sources, inclusive of errors in the observations of the forcing and the carbon fluxes [*Richardson et al.*, 2006] and model assumptions and parameterization, some of the errors are related to the inaccuracy in the prediction of stomatal conductance, which directly affects both simulated LE and photosynthesis and thus creates a relationship between errors in C and errors in latent heat fluxes. Errors in LE are not decoupled from errors in other model-simulated C flux variables. For example, *Dietze et al.* [2011] showed that errors in NEE relate to phenology and vegetative processes at multiple time scales. However, here we focused on the peak growing season to avoid the potential effect of errors in the modeled phenology.

Errors in LE and GPP can also be indicative of errors in the way radiation affects stomatal conductance and carbon flux [*Foken*, 2008; *Huntzinger et al.*, 2012; *Richardson et al.*, 2012; *Schaefer et al.*, 2012]. For example, *Foken* [2008] found that most land-surface observational experiments show consistently lower combined LE and *H* than the available energy (net radiation + soil heat flux), which will result in lower simulated LE and GPP than observed.

3.3. Relationships Between LE Errors and the Surface Energy Budget

Apparent errors in LE can be the result of errors in measurement of LE and not necessarily be indicative of a nonphysical result by the model. Both observation errors in fluxes and errors in energy closure in models will lead to lack of energy closure; i.e., the sum of the fluxes will be smaller (or larger) than the net radiation. The lack of energy closure in eddy-covariance observation, particularly at the subdaily time scale, may be a result of changes of the within canopy heat and humidity storage, unaccounted for ground heat flux, and lateral advective fluxes. A simple assumption driven by conservation of energy, which is at the basis of any land-surface model, is that the net radiation equals the sum of sensible, latent, and soil heat fluxes. We can make the simplifying assumption that during the growing season when leaves are fully expanded, the soil heat flux is low relative to the contribution of latent and sensible heat fluxes and does not vary greatly at a particular site (again, relative to latent and sensible heat fluxes). We can therefore approximate the energy deficit, E_x, as

$$E_x = R_d - \mathrm{LE} - H$$

where R_d is the net radiation at the land surface.

We raise two alternative hypotheses: (1) errors in LE are the results of errors in the partitioning of the surface energy budget into LE and *H*, mostly due to an error in the value of stomatal conductance which leads to overestimation or underestimation of LE and thus a compensation with an underestimation or overestimation of *H* driven by the assumption of conservation of energy in the model and (2) errors in LE are a result of observation or model error in energy closure, and thus, an overall overestimation/underestimation of the total surface fluxes will be distributed to errors in both LE and *H*. In the case of hypothesis (1), we predict that errors in *H* and errors in LE will be negatively correlated, while in the case of (2), the LE and *H* errors should be positively correlated. Additionally, in the case of (1), errors in LE or *H* should not be correlated with the observed E_x, while in the case of (2), both *H* and LE errors (the sum of which defines the error in modeled E_x) should be positively correlated with the observed E_x.

We analyzed the relationship between model errors in LE, model errors in *H*, observed E_x, and modeled E_x during the daytime hours of the growing season (between 9 A.M. and 6 P.M. and when $R_d > 20\ \mathrm{W/m^2}$) and when turbulence mixing is high (above the u^* threshold). In these times, changes of heat or humidity storage in the canopy should be minimal, and these time periods are when transpiration is the major component of LE (Table 3). Errors in LE and errors in *H* were very weakly correlated (all $R^2 < 0.05$) with an inconsistent trend, positive in roughly half of the models and negative in the others (Table 3). Errors in LE and errors in *H* were positively correlated with errors in observed E_x ($R^2 < 0.14$ and 0.14, respectively). Modeled E_x was also positively correlated with observed E_x ($R^2 < 0.33$), indicating that models perform less well when the site observations include a large-energy closure error. The significance, strength, and sign of these correlations show that it is impossible to reject either hypotheses and that model errors are likely a combination of errors in LE that are largely related to model's or observation's ability to close the energy balance and that errors in LE and H are driven by compensation to conserve energy in several of the models we studied. Therefore, we can assume that, at least to some degree, causes of model errors in LE are independent of the energy budget and related to the calculation of transpiration and stomatal conductance.

Table 3. Correlation Statistics Between the Modeled and Observed Energy Budget Deficit (E_x) and Errors in LE and H for Each Model[a]

(y Versus x)	Modeled E_x Versus Observed E_x		LE Error Versus Observed E_x		H Error Versus Observed E_x		LE Error Versus H Error	
Model	R^2	slope	R^2	slope	R^2	slope	R^2	slope
CanIBIS	0.15	0.59	0.01	0.09	0.12	0.32	0.00	−0.06
CN-CLASS	0.28	0.73	0.07	0.19	0.01	0.09	0.01	−0.07
Ecosys	0.24	0.86	0.04	0.15	0.00	−0.01	0.04	0.14
ED2	-	-	0.04	0.35	-	-	-	-
ORCHIDEE	0.22	0.64	0.02	0.13	0.07	0.24	0.00	−0.04
SiB3	0.10	0.38	0.14	0.28	0.13	0.35	0.03	0.13
SibCASA	0.14	0.42	0.12	0.26	0.14	0.32	0.02	0.11
SSiB2	0.33	0.64	0.12	0.24	0.02	0.13	0.05	−0.16
Teco	-	-	0.00	−0.11	-	-	-	-

[a]ED2 and Teco did not provide model outputs of H. All $P < 0.0001$.

3.4. Diurnal Patterns of LE Error and Hysteresis in the LE-VPD Curve

Although the majority of site model pairs tend to produce underestimations of LE, intradaily patterns of errors in LE show both underestimations and overestimations, frequently in a compensatory manner. These diurnal patterns of LE errors, for the most part, tend to be grouped well on the basis of the formulation of stomatal conductance in the different models (Figure 5). ED2, which uses the Leuning [*Leuning*, 1995] formulation, consistently underestimated LE, with most of the underestimation during the early part of the day. As the only model in its class, it is not clear what components of its formulation drive this type of error pattern compared to patterns in other models. Cross-Chain Loran Atmospheric Sounding System (CN-CLASS), Organizing Carbon and Hydrology in Dynamic Ecosystems (ORCHIDEE), and Teco, which use the Ball-Woodrow-Berry (*Ball et al.*, 1987) scheme, tend to underestimate transpiration early in the day and overestimate it during the afternoon and early evening. Similar patterns are shown by Ecosys, which uses the Grant-Black (*Grant et al.*, 2006) scheme and exhibits the smallest overall bias. This error pattern corresponds with the pattern of error we predict to be caused due to the lack of plant hydrodynamics—overestimation of the flux late in the day may be driven by the lack of hydrodynamic restriction of stomatal conductance and therefore photosynthesis due to reduced storage levels and low leaf water potential. Parameterization using the long-term (daily, weekly, and monthly) totals of the water flux adjusts the entire curve downward (assumably through changes to parameters controlling light-use efficiency and reduction of maximal photosynthesis and stomatal conductance) and leads to underestimation of LE in the

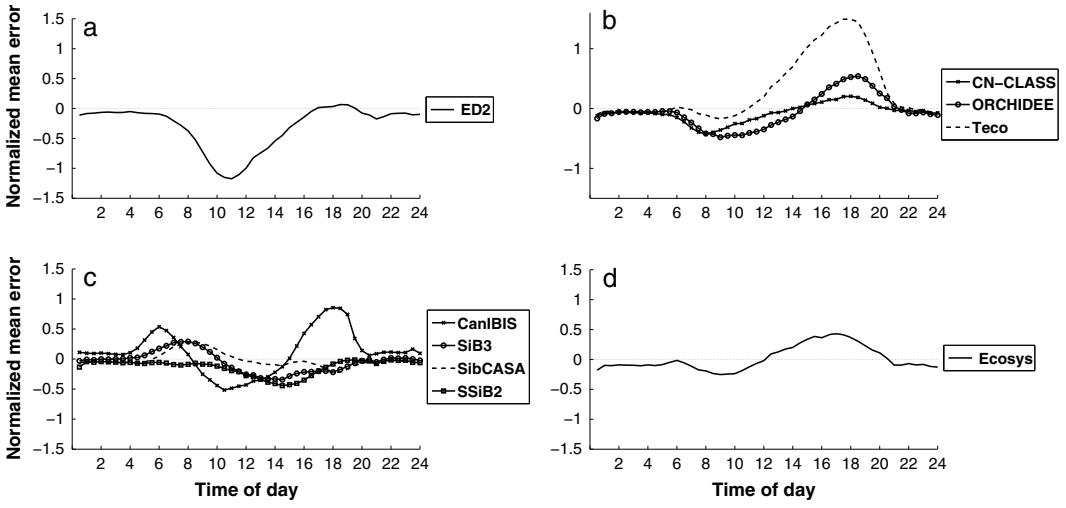

Figure 5. Diurnal model error patterns for specific stomatal conductance schemes. (a) Leuning [*Leuning*, 1995], (b) Ball-Woodrow-Berry (*Ball et al.*, 1987), (c) Collatz-Ball (*Collatz et al.*, 1991), and (d) Grant-Black (*Grant et al.*, 2006).

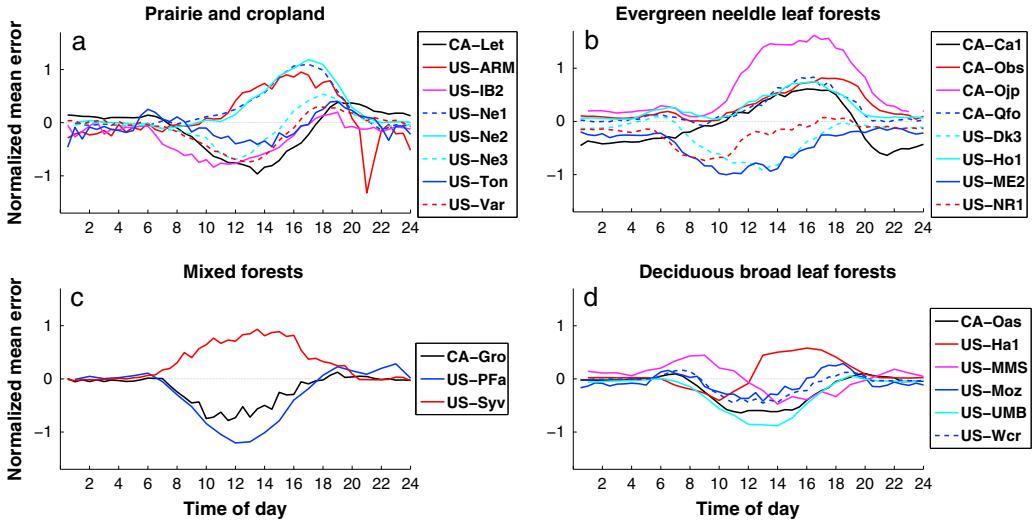

Figure 6. Diurnal average model error patterns for site type. (a) Agricultural, prairie, and grasslands; (b) evergreen needleleaf forests; (c) mixed forests; and (d) deciduous broadleaf forests. Due to the similarity of their error patterns, agricultural (CRO), grassland (GRA), and savanna (WSA) sites were grouped together.

earlier parts of the day. Models using the Collatz-Ball (*Collatz et al.*, 1991) scheme show the inverted patterns and tend to overestimate LE early in the day and then underestimate afternoon LE (Figure 5), which could be caused by an oversensitivity to VPD.

At the site level, the majority of the largest diurnal errors in half hourly LE occurred when the daily average soil conditions were in the range of intermediately wet and when VPD was high (data not shown). The majority of these large errors were underestimations of flux during the hours of 10 A.M. to 3 P.M.. Sites did not tend to demonstrate similar patterns of error throughout the day when grouped by ecosystem type (Figure 6). Regardless of ecosystem type, the majority of sites showed an underestimation of LE during the morning and afternoon followed by an overestimation during the evening. However, some sites (e.g., CA-Let, CA-Gro, US-PFa, US-IB2, US-NR1, US-Dk3, US-Me2, and US-UMB) show an underestimation during the entire day with slight to no overestimation in the evening and nighttime. Other sites show very little error or an overestimation during the early part of the day (e.g., CA-Oas, US-MMS, US-Ton, and US-WCr). Crop sites show the largest intradaily errors, indicating that models have the most difficulty simulating transpiration for these ecosystems.

The underestimation of LE in the first half of the day and overestimation in the second, together with the observation when most models approximate LE very well at the integrated daily time step, demonstrate that model parameterizations offset opposing errors. The largest errors among the four models with the least bias (Ecosys, CN-CLASS, Simple Biosphere/Carnegie-Ames-Stanford Approach (SibCASA), and ORCHIDEE; Figure 2b) occur when the soil is wet and intermediately wet (Figure 3a). The pattern of error indicates that they tend to underestimate evapotranspiration moderately throughout the entire day and more so during the hours of peak transpiration when the soil is wet and intermediately wet. These models tend to overestimate LE when the soil is dry. Conversely, the relatively largest errors for the models with the highest bias (SiB3, CanIBIS, SSiB2, Teco, and ED2; Figure 2b) tend to occur when the soil is dry or intermediately wet (Figure 3b). They show a similar tendency to underestimate LE during peak transpiration but overestimate during the mornings and evenings for all soil conditions. Although nighttime observations of fluxes have larger errors than during the day, due to weak wind and turbulent mixing and thus larger fraction of filtered observations [*Novick et al.*, 2009], the fact that models consistently overestimate nighttime evaporation, rather than fluctuate with larger errors, suggests that at least in part, this nighttime overestimation is driven by parameterization of the models for the total water budget that compensates for underestimation of daytime transpiration. This compensation, particularly during early morning and late evening hours, when transpiration is low, allows models to be reasonably accurate at the overall daily time scale while having consistent bias patterns of the diurnal dynamics.

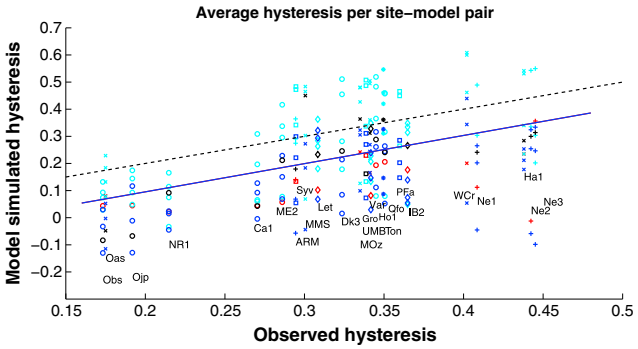

Figure 7. Model-simulated and observed hysteresis for each site model pair with respect to IGBP site classification (ENF (circle), DBF (cross), MF (square), CRO (plus sign), GRA (diamond), and WSA (asterisk) and model's stomatal conductance parameterization (Ball-Woodrow-Berry (*Ball et al.*, 1987)–blue, Collatz-Ball (*Collatz et al.*, 1991)–cyan, Leuning [*Leuning*, 1995]–red, and Grant-Black (*Grant et al.*, 2006)–black). The black dashed line is the 1:1 line, and the blue line is a linear regression, $R^2 = 0.23$, $P < 0.00001$, and slope = 1.039.

The differences between the simulated and observed diurnal dynamics of LE are apparent when analyzed within the framework of the daily hysteresis of LE as a function of VPD. We observed positive hysteresis in all sites in most days (Figure 7). Reversible hysteresis of this type (i.e., the next day can repeat a similar cycle) is usually the result of a numerical reduction to a single dimension of a multidimensional process. There is a debate as to the cause of this hysteresis, whether it is the result of the lag between the daily pattern of VPD and the level of photosynthetic active radiation (PAR) or due to stomatal conductance inherent dependence on the plant hydrodynamics through hydration status at the leaf and branch level [*Tuzet et al.*, 2003; *Verbeeck et al.*, 2007a, 2007b; *Zhang et al.*, 2014]. In the first case, LE is a repeatable function of both VPD and PAR, and the same level of LE is expected when a specific combination of LE and PAR would occur. Hysteresis in the LE curve will be a result of plotting LE as a single-axis function of VPD while ignoring the PAR axis. The daily peak of PAR is earlier than the daily peak of VPD, and thus, higher transpiration levels occur before the daily max of VPD than later in the day. In the case of plant hydrodynamics, LE would be a function of VPD and water storage levels in the plant, as expressed by leaf water potential. Hysteresis may be driven by midday stomata closure [*Brodribb and Holbrook*, 2004; *Sperry et al.*, 2002; *Tyree and Sperry*, 1989; *Tyree and Zimmermann*, 2002]. Water transport from the root is, in most cases, slower than the maximal rate of transpirational water loss from the leaf, and therefore, when storage is depleted, maximal transpiration rates cannot be sustained. Throughout the day, the capacity becomes depleted due to ongoing transpiration. As this hydraulic process occurs, stomata respond to reduced leaf water potential by reducing their aperture. This pattern of stomatal response leads to a decline in the afternoon transpiration relative to the prenoon rates and appears as hysteresis in the LE-VPD curve (Figure 1). In the physical world, LE is a function of VPD, leaf water potential, and PAR, along with other variables (temperature, plant physiology, phenology, etc.), and therefore, it is plausible that the apparent hysteresis is a result of a combination of drivers.

Following our assumptions about the potential sources for the hysteresis, if the source of hysteresis is mostly due to the lag between PAR and VPD, models should be able to resolve the hysteresis well because the stomata parameterizations primarily describe the PAR and VPD response of stomata. In fact, models that overemphasize the role of VPD or PAR in modulating stomatal conductance will predict larger hysteresis than observed. However, the component of the hysteresis that is driven by the lag between VPD-driven stomatal conductance response and plant water storage level will not be resolved by models and thus will lead to lower simulated hysteresis than observed.

Overall, most models tend to underpredict the degree of hysteresis in all sites (Table 4). Underestimation of hysteresis was relatively greater for sites where the observed hysteresis was either very low or very high (Figure 7). Although, for our study, we do not have data available by which to directly calculate plant water status, we use soil water potential as a measure of how much water is available in the soil for root uptake. Similar to the findings of *O'Grady et al.* [2008] and *Chen et al.* [2011], we find that the largest values for observed hysteresis occur when the daily mean VPD is moderate to large, while the smallest occur when VPD is lowest (Table 4). We also find that as observed hysteresis becomes large, model performance declines relative to periods characterized by moderate hysteresis (Figure 7). We suggest that as hysteresis becomes large, it is more dependent on plant hydrodynamic factors than abiotic factors and that this "tailing off" of models' ability to accurately simulate these effects is also related to the lack of a mechanistic manner with which to simulate changing plant water status and the related stomatal closure.

Table 4. Degree of Hysteresis Errors Across Multiple Forcing Conditions, Averaged Over All Sites Studied[a]

	Average Observed Degree of Hysteresis	Error: *Ball et al.* [1987]	Error: *Collatz et al.* [1991]	Error: *Leuning* [1995]	Error: *Grant et al.* [2006]	Grand Averaged Error
All	0.217	−0.183	−0.009	−0.186	−0.106	−0.107
Wet soil	0.214	−0.176	0.002	−0.168	−0.104	−0.097
Low VPD	0.193	−0.202	−0.033	−0.207	−0.131	−0.129
Med soil	0.215	−0.188	−0.026	−0.181	−0.108	−0.116
Med VPD	0.251	−0.157	0.023	−0.155	−0.063	−0.076
Dry soil	0.247	−0.175	0.005	−0.178	−0.071	−0.095
High VPD	0.247	−0.156	0.036	−0.183	−0.030	−0.073

[a]Errors are calculated as modeled-observed.

Evergreen needleleaf forests tended to have the lowest observed degree of hysteresis, while crop sites tended to have the highest (Figure 7). The effects of different components of the conductive system, such as the area of conductive xylem, the xylem maximal conductance and capacitance, the shape of the cavitation curve, the sensitivity of stomata to leaf water potential, as well as the response to foliar abscisic acid all combine to describe the hydrodynamic component of stomatal conductance. In this study, we do not have the observations needed to determine which of these are specifically responsible for the differences between site types. We also cannot fully determine to what degree the errors in the hysteresis are driven by errors in the temporal hydrodynamics or errors in the modeled lag between the timing of max VPD and the timing of max transpiration (as suggested by *Zhang et al.* [2014]). Nonetheless, at a very simplistic level, our observations are consistent with the fact that tall conifer forests (large, low wood density) are expected to have the largest amount of storage per transpiring leaf area and thus encounter less and later daily hydrodynamic restriction of stomatal conductance and therefore lower hysteresis, while crops have the lowest storage per leaf area. These results are further supported by a recent study by *McAdam and Brodribb* [2014] that showed no hysteresis in the coniferous species *Metasequoia glyptostroboides* due to lack of ABA response under evaporative stress.

Models using the Collatz-Ball (*Collatz et al.*, 1991) formulation tended to produce larger than observed hysteresis, while all other model types consistently underestimate hysteresis. None of the models are driven by a mechanistically physical representation of the plant hydrodynamics, and therefore, all are expected to produce at least some degree of underestimation of the hysteresis. We propose that the Collatz–Ball-based models overemphasize the effects of VPD and, as we predicted above, generate an overall overestimation the hysteresis. This is further supported by the fact that all and only these models produce the specific pattern of overestimation of transpiration in the early part of the day, when light is the major driver of stomatal conductance (Figure 5c). In contrast, all other models overestimate stomatal conductance in the later part of the day, as we hypothesize the characteristic pattern of lack of modeled plant hydrodynamics (Figures 5a, 5b, and 5d). It is noteworthy that Ecosys, the only model employing the Grant-Black (*Grant et al.*, 2006) formulation, shows the least amount of overall bias (Figure 2b) in the calculation of LE and has a relatively subtle pattern of diurnal error (Figure 5d). The Grant–Black formulation is distinguished in two ways: (1) it provides no direct link between VPD and g_s, and (2) it is the only formulation to directly employ a diagnostic variable representing the plant water potential that controls the stomata response to water limitations, rather than to use a Jarvis-like or Feddes-like water stress factor, which relates stomatal conductance directly to the soil. By subtly altering the formulation of stomatal conductance to include a slightly more physical approach to link conductance to plant water status, Grant–Black may have made an increase in model accuracy. However, with only one model in our study employing this stomatal formulation, it remains unclear if this is the only factor driving its accuracy.

4. Conclusions

Land-surface models are essential tools for predicting how rising atmospheric CO_2 concentrations and climate change will affect our environment and the ways in which we interpret it. While we found that, overall, models resolve the long-term water budget relatively well, errors in simulated LE were found to be correlated with errors in gross primary productivity and net ecosystem exchange. We suggest that model performance in terms of surface heat fluxes as well as carbon fluxes could be improved by improving the simulation of the latent heat flux, and particularly stomatal conductance. Our results indicate that intradaily patterns of errors in LE as

simulated by current land-surface models are likely driven to some degree by the model's lack of ability to account for the daily hysteretic response of transpiration to VPD. This deficiency along with the patterns of the errors in modeled LE is indicative in most models of missing hydrodynamic responses at the leaf level, which limit accurate predictions of stomatal conductance and therefore transpiration. We propose that the poor representation in present land-surface models of plant hydrodynamic fluctuations stems from the lack of a mechanistic tool with which to simulate water flux from the soil through the vegetative system. In order to improve model robustness, accuracy in the simulation of the subdaily time scale must be achieved.

Overall, at daily, monthly, and seasonal time scales, the models were accurate with model error rates close to the observation uncertainty, which defines the limit of achievable accuracy. Nonetheless, the diurnal pattern of errors at the hourly time scale may accumulate to affect particular large-scale dynamics in weather models. At short time scales, these errors in the modeled LE will lead to errors in model prediction of temperature which will be reflected in simulated *H* and in the response of photosynthesis to temperature and thermal injury [*Dietze*, 2014; *Sage and Kubien*, 2007]. We hypothesize that in areas with strong diurnal patterns of wind, such as places with lake or sea breeze, or mountains with thermally driven slope flows, trading off morningtime transpiration for afternoon transpiration will lead to different advection paths for humidity, which will consequently change the long-term mean humidity downwind of the transpiring vegetation. Cloud formation is another process with a strong diurnal cycle, where differences in the intradaily dynamics of transpiration may affect moisture availability and thermal uplift strength at key times for specific cloud processes [*de Arellano et al.*, 2014; *LeMone and Pennell*, 1976]. Similarly, the diurnal dynamics of stomatal conductance affect processes other than evaporation and photosynthesis. For example, emission rates of some volatile organic compounds (VOCs) from certain species of plants (e.g., *Fagus sylvatica*, *Quercur robur*, *Betula pendula*, and *Eucalyptus camaldulensis*) are dependent on stomatal conductance [*Folkers et al.*, 2008; *Hüve et al.*, 2007; *Niinemets and Reichstein*, 2003; *Winters et al.*, 2009]. The large-scale consequences of these VOC emissions are determined by the reactions and interactions of these VOCs with other chemicals in the atmosphere (e.g., ozone), light availability, and temperature, all of which have strong diurnal dynamics. Therefore, changing the diurnal temporal dynamics of stomatal conductance and VOC emissions may result in nonlinear interactions and drive a large-scale difference in the resulting atmospheric chemistry. We propose that an approach for mechanistic representation of plant water potential and its effects on stomatal conductance at a plot scale is needed to increase accuracy at a subdaily time scale in addition to longer periods of drought, which are predicted to become longer and more frequent across a number of areas with global climate change.

Acknowledgments

We acknowledge the site PIs in the Ameriflux and FluxCanada networks that contributed data to this analysis and model PIs that contributed simulation results. This research was supported by the U.S. Department of Energy awards DE-SC0006708, DE-SC0007041 and Ameriflux National Core Site award through Lawrence Berkeley National Laboratory contract #7096915, and the National Science Foundation grants DEB-0911461 including an REU supplement award for A.M. and additional support by the National Oceanic and Atmospheric Administration award NA11OAR4310190. Data analysis was conducted in part at the Ohio Supercomputer Center, allocation grant PAS0409-4. P.C.S. acknowledges support from the U.S. NSF EF 1241881.

References

Allen, C. D., et al. (2010), A global overview of drought and heat-induced tree mortality reveals emerging climate change risks for forests, *For. Ecol. Manage.*, *259*(4), 660–684.

Arain, M. A., F. M. Yuan, and T. A. Black (2006), Soil-plant nitrogen cycling modulated carbon exchanges in a western temperate conifer forest in Canada, *Agric. For. Meteorol.*, *140*(1–4), 171–192.

Baker, I. T., L. Prihodko, A. S. Denning, M. Goulden, S. Miller, and H. R. da Rocha (2008), Seasonal drought stress in the Amazon: Reconciling models and observations, *J. Geophys. Res.*, *113*, G00B01, doi:10.1029/2007JG000644.

Ball, J. T. (1988), *An Analysis of Stomatal Conductance*, 145 pp., Stanford Univ., Stanford, Calif.

Ball, J. T., I. E. Woodrow, and J. A. Berry (1987), A model predicting stomatal conductance and its contribution to the control of photosynthesis under different environmental conditions, in *Progress in Photosynthesis Research*, edited by J. Biggins, pp. 221–224, Springer, Netherlands.

Barr, A. G., T. A. Black, E. H. Hogg, N. Kljun, K. Morgenstern, and Z. Nesic (2004), Inter-annual variability in the leaf area index of a boreal aspen-hazelnut forest in relation to net ecosystem production, *Agric. For. Meteorol.*, *126*(3–4), 237–255.

Beer, C., et al. (2010), Terrestrial gross carbon dioxide uptake: Global distribution and covariation with climate, *Science*, *329*(5993), 834–838.

Bergeron, O., H. A. Margolis, T. A. Black, C. Coursolle, A. L. Dunn, A. G. Barr, and S. C. Wofsy (2007), Comparison of carbon dioxide fluxes over three boreal black spruce forests in Canada, *Global Change Biol.*, *13*(1), 89–107.

Berry, J. A., D. J. Beerling, and P. J. Franks (2010), Stomata: Key players in the earth system, past and present, *Curr. Opin. Plant Biol.*, *13*(3), 232–239.

Bohrer, G., H. Mourad, T. A. Laursen, D. Drewry, R. Avissar, D. Poggi, R. Oren, and G. G. Katul (2005), Finite element tree crown hydrodynamics model (FETCH) using porous media flow within branching elements: A new representation of tree hydrodynamics, *Water Resour. Res.*, *41*, W11404, doi:10.1029/2005WR004181.

Bradford, J. B., R. A. Birdsey, L. A. Joyce, and M. G. Ryan (2008), Tree age, disturbance history, and carbon stocks and fluxes in subalpine Rocky Mountain forests, *Global Change Biol.*, *14*(12), 2882–2897.

Brodribb, T. J., and H. Cochard (2008), Hydraulic failure defines the recovery and point of death in water-stressed conifers, *Plant Physiol.*, *149*(1), 575–584.

Brodribb, T. J., and N. M. Holbrook (2003), Stomatal closure during leaf dehydration, correlation with other leaf physiological traits, *Plant Physiol.*, *132*(4), 2166–2173.

Brodribb, T. J., and N. M. Holbrook (2004), Stomatal protection against hydraulic failure: A comparison of coexisting ferns and angiosperms, *New Phytol.*, *162*(3), 663–670.

Brodribb, T. J., and N. M. Holbrook (2006), Declining hydraulic efficiency as transpiring leaves desiccate: Two types of response, *Plant Cell Environ.*, *29*(12), 2205–2215.
Brodribb, T. J., and N. M. Holbrook (2007), Forced depression of leaf hydraulic conductance in situ: Effects on the leaf gas exchange of forest trees, *Funct. Ecol.*, *21*(4), 705–712.
Campbell, G. S., and J. M. Norman (1998), *An Introduction to Environmental Biophysics*, 2nd ed., pp. xxi+286, Springer-Verlag, Berlin, Germany; Springer-Verlag New York, Inc., New York, N. Y.
Chen, L. X., Z. Q. Zhang, Z. D. Li, J. W. Tang, P. Caldwell, and W. J. Zhang (2011), Biophysical control of whole tree transpiration under an urban environment in Northern China, *J. Hydrol.*, *402*(3–4), 388–400, doi:10.1016/j.jhydrol.2011.03.034.
Choat, B., et al. (2012), Global convergence in the vulnerability of forests to drought, *Nature*, *491*(7426), 752–756.
Collatz, G. J., J. T. Ball, C. Grivet, and J. A. Berry (1991), Pysiological and environmental regulation of stomatal conductance, photosyntesis and transpiration: A model that includes a laminal boundary layer, *Agric. For. Meteorol.*, *54*(2–4), 107–136, doi:10.1016/0168-1923(91)90002-8.
Cook, B. D., et al. (2004), Carbon exchange and venting anomalies in an upland deciduous forest in northern Wisconsin, USA, *Agric. For. Meteorol.*, *126*(3–4), 271–295.
Damour, G., T. Simonneau, H. Cochard, and L. Urban (2010), An overview of models of stomatal conductance at the leaf level, *Plant Cell Environ.*, *33*, 1419–1438.
Davis, K. J., P. S. Bakwin, C. X. Yi, B. W. Berger, C. L. Zhao, R. M. Teclaw, and J. G. Isebrands (2003), The annual cycles of CO_2 and H_2O exchange over a northern mixed forest as observed from a very tall tower, *Global Change Biol.*, *9*(9), 1278–1293.
de Arellano, J. V. G., H. G. Ouwersloot, D. Baldocchi, and C. M. J. Jacobs (2014), Shallow cumulus rooted in photosynthesis, *Geophys. Res. Lett.*, *41*, 1796–1802, doi:10.1002/2014GL059279.
De Kauwe, M. G., et al. (2013), Forest water use and water use efficiency at elevated CO_2: A model-data intercomparison at two contrasting temperate forest FACE sites, *Global Change Biol.*, *19*(6), 1759–1779.
Desai, A. R., P. V. Bolstad, B. D. Cook, K. J. Davis, and E. V. Carey (2005), Comparing net ecosystem exchange of carbon dioxide between an old-growth and mature forest in the upper Midwest, USA, *Agric. For. Meteorol.*, *128*(1–2), 33–55.
Dietze, M. C. (2014), Gaps in knowledge and data driving uncertainty in models of photosynthesis, *Photosynth. Res.*, *119*(1–2), 3–14.
Dietze, M. C., et al. (2011), Characterizing the performance of ecosystem models across time scales: A spectral analysis of the North American Carbon Program site-level synthesis, *J. Geophys. Res.*, *116*, G04029, doi:10.1029/2011JG001661.
Egea, G., A. Verhoef, and P. L. Vidale (2011), Towards an improved and more flexible representation of water stress in coupled photosynthesis–stomatal conductance models, *Agric. For. Meteorol.*, *151*(10), 1370–1384.
Feddes, R. A., P. Kowalik, K. Kolinska-Malinka, and H. Zarandy (1976), Simulation of field water uptake by plants using a soil water dependent root extraction function, *J. Hydrol.*, *31*, 13–26.
Fischer, M. L., D. P. Billesbach, J. A. Berry, W. J. Riley, and M. S. Torn (2007), Spatiotemporal variations in growing season exchanges of CO_2, H_2O, and sensible heat in agricultural fields of the Southern Great Plains, *Earth Interact.*, *11*(17), 1–21, doi:10.1175/EI231.1.
Fisher, J. B., T. A. DeBiase, Y. Qi, M. Xu, and A. H. Goldstein (2005), Evapotranspiration models compared on a Sierra Nevada forest ecosystem, *Environ. Modell. Software*, *20*(6), 783–796.
Flanagan, L. B., L. A. Wever, and P. J. Carlson (2002), Seasonal and interannual variation in carbon dioxide exchange and carbon balance in a northern temperate grassland, *Global Change Biol.*, *8*(7), 599–615.
Foken, T. (2008), The energy balance closure problem: An overview, *Ecol. Appl.*, *18*(6), 1351–1367.
Folkers, A., K. Huve, C. Ammann, T. Dindorf, J. Kesselmeier, E. Kleist, U. Kuhn, R. Uerlings, and J. Wildt (2008), Methanol emissions from deciduous tree species: Dependence on temperature and light intensity, *Plant biol. (Stuttgart, Germany)*, *10*(1), 65–75.
Ford, C. R., R. M. Hubbard, B. D. Kloeppel, and J. M. Vose (2007), A comparison of sap flux-based evapotranspiration estimates with catchment-scale water balance, *Agric. For. Meteorol.*, *145*(3–4), 176–185.
Garrity, S. R., K. Meyer, K. D. Maurer, B. Hardiman, and G. Bohrer (2012), Estimating plot-level tree structure in a deciduous forest by combining allometric equations, spatial wavelet analysis and airborne LiDAR, *Remote Sens. Lett.*, *3*(5), 443–451.
Gough, C. M., B. S. Hardiman, L. E. Nave, G. Bohrer, K. D. Maurer, C. S. Vogel, K. J. Nadelhoffer, and P. S. Curtis (2013), Sustained carbon uptake and storage following moderate disturbance in a Great Lakes forest, *Ecol. Appl.*, *23*(5), 1202–1215.
Grant, R. F., T. A. Black, D. Gaumont-Guay, N. Kljun, A. G. Barrc, K. Morgenstern, and Z. Nesic (2006), Net ecosystem productivity of boreal aspen forests under drought and climate change: Mathematical modelling with Ecosys, *Agric. For. Meteorol.*, *140*(1–4), 152–170, doi:10.1016/j.agrformet.2006.01.012.
Griffis, T. J., T. A. Black, K. Morgenstern, A. G. Barr, Z. Nesic, G. B. Drewitt, D. Gaumont-Guay, and J. H. McCaughey (2003), Ecophysiological controls on the carbon balances of three southern boreal forests, *Agric. For. Meteorol.*, *117*(1–2), 53–71.
Gu, L., T. Meyers, S. G. Pallardy, P. J. Hanson, B. Yang, M. Heuer, K. P. Hosman, J. S. Riggs, D. Sluss, and S. D. Wullschleger (2006), Direct and indirect effects of atmospheric conditions and soil moisture on surface energy partitioning revealed by a prolonged drought at a temperate forest site, *J. Geophys. Res.*, *111*, D16102, doi:10.1029/2006JD007161.
Hickler, T., I. C. Prentice, B. Smith, M. T. Sykes, and S. Zaehle (2006), Implementing plant hydraulic architecture within the LPJ Dynamic Global Vegetation Model, *Global Ecol. Biogeogr.*, *15*(6), 567–577.
Huntington, T. G., A. D. Richardson, K. J. McGuire, and K. Hayhoe (2009), Climate and hydrological changes in the northeastern United States: Recent trends and implications for forested and aquatic ecosystems, *Can. J. For. Res.*, *39*(2), 199–212.
Huntzinger, D. N., et al. (2012), North American Carbon Program (NACP) regional interim synthesis: Terrestrial biospheric model intercomparison, *Ecol. Model.*, *232*, 144–157.
Hüve, K., M. M. Christ, E. Kleist, R. Uerlings, Ü. Niinemets, A. Walter, and J. Wildt (2007), Simultaneous growth and emission measurements demonstrate an interactive control of methanol release by leaf expansion and stomata, *J. Exp. Bot.*, *58*(7), 1783–1793.
Janott, M., S. Gayler, A. Gessler, M. Javaux, C. Klier, and E. Priesack (2011), A one-dimensional model of water flow in soil-plant systems based on plant architecture, *Plant Soil*, *341*(1–2), 233–256.
Jarvis, P. G. (1976), The interpretation of the variations in leaf water potential and stomatal conductance found in canopies in the field, *Philos. Trans. R. Soc. B-Biol. Sci.*, *273*, 593–610.
Jasechko, S., Z. D. Sharp, J. J. Gibson, S. J. Birks, Y. Yi, and P. J. Fawcett (2013), Terrestrial water fluxes dominated by transpiration, *Nature*, *496*(7445), 347–350, doi:10.1038/nature11983.
Katul, G. G., R. Oren, S. Manzoni, C. Higgins, and M. B. Parlange (2012), Evapotranspiration: A process driving mass transport and energy exchange in the soil-plant-atmosphere-climate system, *Rev. Geophys.*, *50*, RG3002, doi:10.1029/2011RG000366.
Kucharik, C. J., J. A. Foley, C. Delire, V. A. Fisher, M. T. Coe, J. D. Lenters, C. Young-Molling, N. Ramankutty, J. M. Norman, and S. T. Gower (2000), Testing the performance of a dynamic global ecosystem model: Water balance, carbon balance, and vegetation structure, *Global Biogeochem. Cycle*, *14*(3), 795–825.

LeMone, M. A., and W. T. Pennell (1976), The relationship of trade wind cumulus distribution to subcloud layer fluxes and structure, *Mon. Weather Rev.*, *104*(5), 524–539.
Leuning, R. (1995), A critical appraisal of a combined stomatal-photosynthesis model for C3 plants, *Plant Cell Environ.*, *18*, 339–355.
Ma, S. Y., D. D. Baldocchi, L. K. Xu, and T. Hehn (2007), Inter-annual variability in carbon dioxide exchange of an oak/grass savanna and open grassland in California, *Agric. For. Meteorol.*, *147*(3–4), 157–171.
McAdam, S. A. M., and T. J. Brodribb (2014), Separating active and passive influences on stomatal control of transpiration, *Plant Physiol.*, *164*(4), 1578–1586.
McCaughey, J. H., M. R. Pejam, M. A. Arain, and D. A. Cameron (2006), Carbon dioxide and energy fluxes from a boreal mixedwood forest ecosystem in Ontario, Canada, *Agric. For. Meteorol.*, *140*(1–4), 79–96.
McCulloh, K. A., and J. S. Sperry (2005), Patterns in hydraulic architecture and their implications for transport efficiency, *Tree Physiol.*, *25*, 257–267.
McCulloh, K. A., D. M. Johnson, F. C. Meinzer, S. L. Voelker, B. Lachenbruch, and J.-C. Domec (2012), Hydraulic architecture of two species differing in wood density: Opposing strategies in co-occurring tropical pioneer trees, *Plant Cell Environ.*, *35*(1), 116–125.
Medvigy, D., S. C. Wofsy, J. W. Munger, D. Y. Hollinger, and P. R. Moorcroft (2009), Mechanistic scaling of ecosystem function and dynamics in space and time: Ecosystem Demography model version 2, *J. Geophys. Res.*, *114*, G01002, doi:10.1029/2008JG000812.
Nave, L. E., et al. (2011), Disturbance and the resilience of coupled carbon and nitrogen cycling in a north temperate forest, *J. Geophys. Res.*, *116*, G04016, doi:10.1029/2011JG001758.
Niinemets, Ü., and M. Reichstein (2003), Controls on the emission of plant volatiles through stomata: Differential sensitivity of emission rates to stomatal closure explained, *J. Geophys. Res.*, *108*(D7), 4208, doi:10.1029/2002JD002620.
Niyogi, D., K. Alapaty, S. Raman, and F. Chen (2009), Development and evaluation of a coupled photosynthesis-based gas exchange evapotranspiration model (GEM) for mesoscale weather forecasting applications, *J. Appl. Meteorol. Climatol.*, *48*(2), 349–368.
Novick, K. A., R. Oren, P. C. Stoy, M. B. S. Siqueira, and G. G. Katul (2009), Nocturnal evapotranspiration in eddy-covariance records from three co-located ecosystems in the Southeastern US: Implications for annual fluxes, *Agric. For. Meteorol.*, *149*(9), 1491–1504.
O'Grady, A. P., D. Worledge, and M. Battaglia (2008), Constraints on transpiration of *Eucalyptus globulus* in southern Tasmania, Australia, *Agric. For. Meteorol.*, *148*(3), 453–465, doi:10.1016/j.agrformet.2007.10.006.
Oishi, A. C., R. Oren, and P. C. Stoy (2008), Estimating components of forest evapotranspiration: A footprint approach for scaling sap flux measurements, *Agric. For. Meteorol.*, *148*(11), 1719–1732.
Pan, Y., et al. (2011), A large and persistent carbon sink in the world's forests, *Science*, *333*(6045), 988–993.
Phillips, N. G., M. G. Ryan, B. J. Bond, N. G. McDowell, T. M. Hinckley, and J. Cermak (2003), Reliance on stored water increases with tree size in three species in the Pacific Northwest, *Tree Physiol.*, *23*(4), 237–245.
Post, W. M., R. C. Izaurralde, J. D. Jastrow, B. A. McCarl, J. E. Amonette, V. L. Bailey, P. M. Jardine, T. O. West, and J. Z. Zhou (2004), Enhancement of carbon sequestration in US soils, *BioScience*, *54*(10), 895–908.
Rawls, W. J., D. L. Brakensiek, and K. E. Saxton (1982), Estimation of soil water properties, *Trans. ASAE*, *25*(5), 1316–1328.
Reichstein, M., et al. (2005), On the separation of net ecosystem exchange into assimilation and ecosystem respiration: Review and improved algorithm, *Global Change Biol.*, *11*(9), 1424–1439.
Richardson, A. D., et al. (2006), A multi-site analysis of random error in tower-based measurements of carbon and energy fluxes, *Agric. For. Meteorol.*, *136*(1–2), 1–18.
Richardson, A. D., D. Y. Hollinger, D. B. Dail, J. T. Lee, J. W. Munger, and J. O'Keefe (2009), Influence of spring phenology on seasonal and annual carbon balance in two contrasting New England forests, *Tree Physiol.*, *29*(3), 321–331.
Richardson, A. D., et al. (2012), Terrestrial biosphere models need better representation of vegetation phenology: Results from the North American Carbon Program Site Synthesis, *Global Change Biol.*, *18*(2), 566–584.
Sage, R. F., and D. S. Kubien (2007), The temperature response of C-3 and C-4 photosynthesis, *Plant Cell Environ.*, *30*(9), 1086–1106.
Savabi, M. R., and C. O. Stockle (2001), Modeling the possible impact of increased CO_2 and temperature on soil water balance, crop yield and soil erosion, *Environ. Modell. Software*, *16*(7), 631–640.
Schaefer, K., G. J. Collatz, P. Tans, A. S. Denning, I. Baker, J. Berry, L. Prihodko, N. Suits, and A. Philpott (2008), Combined Simple Biosphere/Carnegie-Ames-Stanford Approach terrestrial carbon cycle model, *J. Geophys. Res.*, *113*, G03034, doi:10.1029/2007JG000603.
Schaefer, K., et al. (2012), A model-data comparison of gross primary productivity: Results from the North American Carbon Program site synthesis, *J. Geophys. Res.*, *117*, G03010, doi:10.1029/2012JG001960.
Schmid, H. P., C. S. B. Grimmond, F. Cropley, B. Offerle, and H. B. Su (2000), Measurements of CO_2 and energy fluxes over a mixed hardwood forest in the mid-western United States, *Agric. For. Meteorol.*, *103*(4), 357–374.
Schwalm, C. R., T. A. Black, K. Morgenstern, and E. R. Humphreys (2007), A method for deriving net primary productivity and component respiratory fluxes from tower-based eddy covariance data: A case study using a 17-year data record from a Douglas-fir chronosequence, *Global Change Biol.*, *13*(2), 370–385.
Schwalm, C. R., et al. (2010), A model-data intercomparison of CO_2 exchange across North America: Results from the North American Carbon Program site synthesis, *J. Geophys. Res.*, *115*, G00H05, doi:10.1029/2009JG001229.
Sellers, P. J., M. D. Heiser, F. G. Hall, S. J. Goetz, D. E. Strebel, S. B. Verma, R. L. Desjardins, P. M. Schuepp, and J. I. MacPherson (1995), Effects of spatial variability in topography, vegetation cover and soil moisture on area-averaged surface fluxes: A case study using the FIFE 1989 data, *J. Geophys. Res.*, *100*(D12), 25,607–25,629, doi:10.1029/95JD02205.
Siqueira, M. B., G. G. Katul, D. A. Sampson, P. C. Stoy, J. Y. Juang, H. R. McCarthy, and R. Oren (2006), Multiscale model intercomparisons of CO_2 and H_2O exchange rates in a maturing southeastern US pine forest, *Global Change Biol.*, *12*(7), 1189–1207.
Sperry, J. S., U. G. Hacke, R. Oren, and J. P. Comstock (2002), Water deficits and hydraulic limits to leaf water supply, *Plant Cell Environ.*, *25*(2), 251–263.
Stoy, P. C., G. G. Katul, M. B. S. Siqueira, J.-Y. Juang, K. A. Novick, H. R. McCarthy, A. C. Oishi, J. M. Uebelherr, H.-S. Kim, and R. Oren (2006), Separating the effects of climate and vegetation on evapotranspiration along a successional chronosequence in the southeastern US, *Global Change Biol.*, *12*(11), 2115–2135.
Stoy, P. C., et al. (2013), Evaluating the agreement between measurements and models of net ecosystem exchange at different times and time scales using wavelet coherence: An example using data from the North American Carbon Program Site-Level Interim Synthesis, *Biogeosci. Discuss.*, *10*(2), 3039–3077.
Thomas, C. K., B. E. Law, J. Irvine, J. G. Martin, J. C. Pettijohn, and K. J. Davis (2009), Seasonal hydrology explains interannual and seasonal variation in carbon and water exchange in a semiarid mature ponderosa pine forest in central Oregon, *J. Geophys. Res.*, *114*, G04006, doi:10.1029/2009JG001010.
Thomsen, J., G. Bohrer, A. M. Matheny, V. Y. Ivanov, L. He, H. Renninger, and K. Schäfer (2013), Contrasting hydraulic strategies during dry soil conditions in *Quercus rubra* and *Acer rubrum* in a sandy site in Michigan, *Forests*, *4*(4), 1106–1120.

Tuzet, A., A. Perrier, and R. Leuning (2003), A coupled model of stomatal conductance, photosynthesis and transpiration, *Plant Cell Environ.*, *26*, 1097–1116.

Tyree, M. T., and J. S. Sperry (1989), Vulnerability of xylem to cavitation and embolism, *Annu. Rev. Plant Physiol. Plant Mol. Biol*, *40*, 19–36.

Tyree, M. T., and M. H. Zimmermann (2002), Xylem structure and the ascent of sap, in *Xylem Structure and the Ascent of Sap*, edited, p. i, Springer-Verlag New York Inc., New York, NY; Springer-Verlag GmbH & Co. KG, Berlin, Germany.

Urbanski, S., C. Barford, S. Wofsy, C. Kucharik, E. Pyle, J. Budney, K. McKain, D. Fitzjarrald, M. Czikowsky, and J. W. Munger (2007), Factors controlling CO_2 exchange on timescales from hourly to decadal at Harvard Forest, *J. Geophys. Res.*, *112*, G02020, doi:10.1029/2006JG000293.

Verbeeck, H., K. Steppe, N. Nadezhdina, M. O. De Beeck, G. Deckmyn, L. Meiresonne, R. Lemeur, J. Cermak, R. Ceulemans, and I. A. Janssens (2007a), Model analysis of the effects of atmospheric drivers on storage water use in Scots pine, *Biogeosciences*, *4*(4), 657–671.

Verbeeck, H., K. Steppe, N. Nadezhdina, M. Op de Beeck, G. Deckmyn, L. Meiresonne, R. Lemeur, J. Cermak, R. Ceulemans, and I. A. Janssens (2007b), Stored water use and transpiration in Scots pine: A modeling analysis with ANAFORE, *Tree Physiol.*, *27*(12), 1671–1685.

Verbeeck, H., P. Peylin, C. Bacour, D. Bonal, K. Steppe, and P. Ciais (2011), Seasonal patterns of CO_2 fluxes in Amazon forests: Fusion of eddy covariance data and the ORCHIDEE model, *J. Geophys. Res.*, *116*, G02018, doi:10.1029/2010JG001544.

Verma, S. B., et al. (2005), Annual carbon dioxide exchange in irrigated and rainfed maize-based agroecosystems, *Agric. For. Meteorol.*, *131*(1–2), 77–96.

Weng, E., and Y. Luo (2008), Soil hydrological properties regulate grassland ecosystem responses to multifactor global change: A modeling analysis, *J. Geophys. Res.*, *113*, G03003, doi:10.1029/2007JG000539.

Winters, A. J., M. A. Adams, T. M. Bleby, H. Rennenberg, D. Steigner, R. Steinbrecher, and J. Kreuzwieser (2009), Emissions of isoprene, monoterpene and short-chained carbonyl compounds from *Eucalyptus* spp. in southern Australia, *Atmos. Environ.*, *43*(19), 3035–3043.

Wu, Y. P., S. G. Liu, and O. I. Abdul-Aziz (2012), Hydrological effects of the increased CO_2 and climate change in the Upper Mississippi River Basin using a modified SWAT, *Clim. Change*, *110*(3–4), 977–1003.

Zhang, Q., S. Manzoni, G. Katul, A. Porporato, and D. Yang (2014), The hysteretic evapotranspiration—Vapor pressure deficit relation, *J. Geophys. Res. Biogeosci.*, *119*, 125–140, doi:10.1002/2013JG002484.

Zimmerman, M. H. (1983), *Xylem Structure and the Ascent of Sap*, 125 pp., Springer-Verlag, Berlin.